

## Analysis of cross-talk effects in volume holographic interconnections using perturbative integral expansion method

Sang Kyu Jin

*Department of Electrical Engineering, Yeongdong College,  
Kangnung, 210-840 KOREA  
Tel: +82-391-610-0328, Fax: +82-391-44-8809*

(Received May 28, 1998)

Cross-talk effects in high-density volume holographic interconnections are investigated using perturbative iteration method of the integral form of Maxwell's wave equation. In this method, the paraxial approximation and negligence of backward scattering introduced in conventional coupled mode theory is not assumed. Interaction geometries consisting of non-coplanar light waves and multiple index gratings are studied. Arbitrary light polarization is considered. Systematic analysis of cross-talk effects due to multiple index gratings is performed in increasing level of diffraction orders corresponding to successive iterations. Some numerical examples are given for first and third order diffraction.

### I. INTRODUCTION

Optical interconnection elements can potentially act as a powerful alternative to electrical wiring in neural network implementation because photons lack the interactive nature of electrons. As a result, photonic interconnections offer minimal signal deterioration, immunity to parasitic loading, and insensitivity to electromagnetic interference(EMI), among other advantages. However, the low capacity of thin hologram interconnections can be a severe problem if a global interconnection is needed between a very large number of input and output pixels in the case of associative memory and learning neural networks. To overcome the shortcomings of conventional interconnection methods, a volume holographic interconnection scheme has been proposed[1,2]. This scheme is based on storing one grating distributed in the whole volume for every pair of input and output pixels as shown in Fig. 1. The volume holographic interconnections exploit the third spatial dimension by using angular selectivity to store the interconnection patterns. The potential for a dramatic increase in the storage capacity offered by volume holograms was recognized early on by Van Heerden[3]. To ensure independent interconnects, cross-talk effects have been investigated by using a simple coupled mode theory[4-6]. The first order cross-talk effect has been minimized by eliminating identical redundant gratings between input and output pixels, and a specific input and output pattern was devised to minimize the first order cross-talk effect[2]. The noise of the volume holographic interconnections was iden-

tified as coming from third order diffraction[2]. The explicit formula for the signal-to-noise ratio was obtained by using a simple coupled mode theory under the assumption of isotropic and coplanar light diffraction from superposed volume gratings[2]. However, in a real situation, anisotropic light diffraction from non-coplanar superposed volume gratings should be considered to analyze the cross-talk effects.

In this paper, we use a rigorous method of perturbative integral expansion to study cross-talk effects in superposed volume gratings. This method can be applied to an arbitrary interaction geometry of optical waves and volume index gratings. It also accounts for backward as well as forward diffraction simultaneously. In section II, a brief summary of the perturbative integral expansion method is introduced. In section III, cross-talk effects of the first, second, and the third level diffraction are analyzed. Some numerical results are presented in section IV. Finally, conclusions are described.

### II. GENERAL FORMULA OF MULTIPLE LIGHT DIFFRACTION

A brief summary of the perturbative integral expansion method as applied to the wave diffraction by multiple gratings is presented. The interaction geometry between light waves and volume gratings consists of an infinite slab bounded by  $z = 0$  and  $z = d$ . Anisotropic host materials and anisotropic volume index gratings are considered in general. The macro-

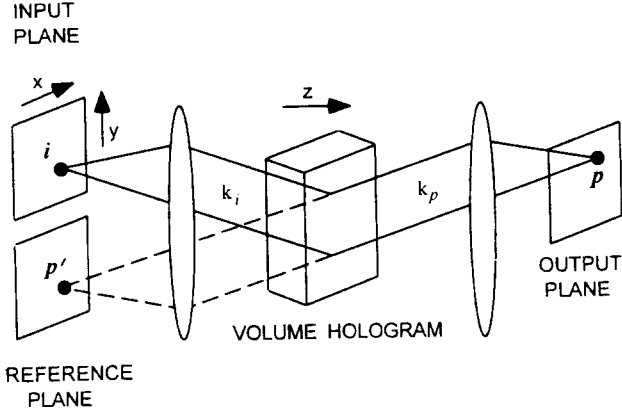


FIG. 1. Diagram showing volume holographic interconnection between input pixel  $i$  and output pixel  $p$ . To make the interconnection, a grating generated by interfering light waves emanating from pixels  $i$  and  $p'$  is stored and read by the light coming from the pixel  $i$ .

scopic polarization is given by

$$\mathbf{P}(\mathbf{r}, t) = \varepsilon_0 \chi \mathbf{E}(\mathbf{r}, t) + \varepsilon_0 \gamma(\mathbf{r}) \mathbf{E}(\mathbf{r}, t), \quad (1)$$

where  $\varepsilon_0$  is the permittivity of the vacuum,  $\chi$  is the susceptibility tensor of the anisotropic host material.  $\gamma(\mathbf{r})$  is a second rank tensor describing the perturbation caused by anisotropic volume gratings, and thus it is zero outside the slab. In the case of multiplexed volume gratings, the perturbation  $\gamma(\mathbf{r})$  consists of a sum of sinusoidal refractive index gratings. Maxwell's wave equation for monochromatic light waves with frequency  $\omega$  in MKS units reads

$$(\nabla^2 - \text{graddiv} + k_0^2 \varepsilon) \mathbf{E} = -k_0^2 \gamma \mathbf{E}, \quad (2)$$

where  $\varepsilon = 1 + \chi$  and  $k_0 = \omega/c$ . We assumed that the

material is non magnetic and there is no free charge. Defining a Green's function for Eq.(2) as

$$(\nabla^2 - \text{graddiv} + k_0^2 \varepsilon) g(\mathbf{r}, \mathbf{r}') = -\mathbf{I} \delta(\mathbf{r} - \mathbf{r}'), \quad (3)$$

where  $\mathbf{I}$  is a unit matrix and  $g$  is a second rank tensor, then, the integral representation of Eq.(2) is given by

$$\mathbf{E}(\mathbf{r}) = \mathbf{E}_0 \exp[i\mathbf{k} \cdot \mathbf{r}] + k_0^2 \int d\mathbf{r}' g(\mathbf{r}, \mathbf{r}') \gamma(\mathbf{r}') \mathbf{E}(\mathbf{r}'), \quad (4)$$

where  $\mathbf{r}'$  denotes the secondary source position vector which ranges over all the points inside the slab. If we iterate Eq.(4), we obtain the perturbative integral expansion

$$\mathbf{E}(\mathbf{r}) = \sum_{n=0}^{\infty} \mathbf{E}^{(n)}(\mathbf{r}), \quad (5)$$

where  $\mathbf{E}^{(0)}$  is the incident plane wave, and an individual diffracted component at the  $n$ -th level is given by [7,8]

$$\mathbf{E}^{(n)}(\mathbf{r}) = \sum_{\beta_n=a}^d S_n^{\beta_n} \Phi_n^{\beta_n} \mathbf{E}_0 \exp(i\mathbf{k}_n^{\beta_n} \cdot \mathbf{r}), \quad (6)$$

where,

$$S_n^{\beta_n} = \frac{1}{(\varepsilon_{zz})^n} s(\beta_n) \sum_{\beta_{n-1}=a}^d \sum_{\beta_{n-2}=a}^d \cdots \sum_{\beta_1=a}^d \frac{1}{\prod_n^{\beta_n} \prod_{n-1}^{\beta_{n-1}} \cdots \prod_1^{\beta_1}} \quad (7)$$

$$\begin{cases} s(\beta_n) = 1 & \text{for } \beta_n = a, b \\ s(\beta_n) = -1 & \text{for } \beta_n = c, d \end{cases}$$

and the phase correlation function  $\Phi$  is defined as

$$\begin{aligned} \Phi_n^{\beta_n} = & -\mathbf{A}(\mathbf{k}_n^{\beta_n}) \prod_{q=n-1}^1 \mathbf{A}(\mathbf{k}_q) \cdot \frac{1 - \exp(-iP_n^{\beta_n} d)}{P_n^{\beta_n} \prod_{q=1}^{n-1} P_q^{\beta_q}} \\ & + (-1)^{n-1} \sum_{q=1}^{n-1} \mathbf{A}(\mathbf{k}_n^{\beta_n}) \prod_{h=n-1}^q \mathbf{A}(\mathbf{K}_h + P_q^{\beta_q} \hat{z}) \cdot f_q(\beta_q) \cdot \frac{1 - \exp\{i(P_n^{\beta_n} - P_q^{\beta_q})d\}}{P_q^{\beta_q} (P_q^{\beta_q} - P_n^{\beta_n}) \prod_{h=1, h \neq q}^{n-1} (P_q^{\beta_q} - P_h^{\beta_h})}. \end{aligned} \quad (8)$$

$f_q(\beta_q)$  for  $q > 1$  in Eq.(8) is obtained by using the following formulas:

$$f_q(\beta_q) = (-1)^{q-1} \frac{\prod_{h=q-1}^1 \mathbf{A}(\mathbf{k}_h) (P_q^{\beta_q} - P_h^{\beta_h})}{\prod_{h=1}^{q-1} P_h^{\beta_h}} - \sum_{t=1}^{q-1} \left[ \frac{P_q^{\beta_q} \prod_{h=q-1}^t \mathbf{A}(\mathbf{k}_h - P_t^{\beta_t} \hat{z}) \prod_{h=1}^{q-1} (P_q^{\beta_q} - P_h^{\beta_h})}{P_t^{\beta_t} \prod_{h=1, h \neq t}^q (P_t^{\beta_t} - P_h^{\beta_h})} \cdot f_t(\beta_t) \right] \quad \text{for } \beta_q = a, b, \quad (9)$$

$$f_q(\beta_q) = \left[ (-1)^{q-1} \frac{\prod_{h=q-1}^1 \mathbf{A}(\mathbf{k}_h) (P_q^{\beta_q} - P_h^{\beta_h})}{\prod_{h=1}^{q-1} P_h^{\beta_h}} - \sum_{t=1}^{q-1} \frac{P_q^{\beta_q} \prod_{h=q-1}^t \mathbf{A}(\mathbf{k}_h - P_t^{\beta_t} \hat{z}) \prod_{h=1}^{q-1} (P_q^{\beta_q} - P_h^{\beta_h})}{P_t^{\beta_t} \prod_{h=1, h \neq t}^q (P_t^{\beta_t} - P_h^{\beta_h})} \cdot g_t(\beta_t) \right] \cdot e^{-iP_q^{\beta_q} d} \quad \text{for } \beta_q = c, d, \quad (10)$$

where  $g_q(\beta_q) = f_q(\beta_q) \exp(ik_q^{\beta_q} d)$  for all  $q$ , (11)

$$\begin{cases} f_1(\beta_1) = 1 & \text{for } \beta_1 = a, b \\ f_1(\beta_1) = \exp(-ip_1^{\beta_1} d) & \text{for } \beta_1 = c, d, \end{cases} \quad (12)$$

$$\Pi_j^{\beta_j} = \prod_{\beta_i = a, \beta_i \neq \beta_j}^d (u_j^{\beta_j} - u_i^{\beta_i}), \quad (13)$$

$$P_j^{\beta_j} = u_j^{\beta_j} - k_{jz} = u_j^{\beta_j} - (k_z + \sum_{t=1}^j \mathbf{K}_{tz}), \quad (14)$$

$$\mathbf{k}_j^{\beta_j} = k_{jx} \hat{x} + k_{jy} \hat{y} + u_j^{\beta_j} \hat{z}, \quad (15)$$

$$\mathbf{A}(\mathbf{k}_n^{a,b}) = \text{Ad}(k_{nx}, k_{ny}, u_n^{a,b}) \alpha_n. \quad (16)$$

Then, Fourier representation  $G(\mathbf{q})$  of the Green's function  $g(\mathbf{r}, \mathbf{r}')$  in Eq.(3) can be written as  $\text{Ad}(\mathbf{q})/D(\mathbf{q})$ , where  $D(\mathbf{q})$  and  $\text{Ad}(\mathbf{q})$  are determinant and adjoint matrix respectively. Now,  $D(\mathbf{q})$  and  $\text{Ad}_{ij}(\mathbf{q})$  in the coordinate system where dielectric tensor  $\varepsilon$  is diagonalized are given by [8]

$$D(\mathbf{q}) = k_0^2 [q_z^2 + (q_x^2 + q_y^2) - k_0^2 \varepsilon_{xx}] \times [\varepsilon_{zz} q_z^2 + \varepsilon_{xx} (q_x^2 + q_y^2) - k_0^2 \varepsilon_{xx} \varepsilon_{zz}], \quad (17)$$

$$\begin{aligned} \text{Ad}_{11} &= q_z^2 (q_x^2 - k_0^2 \varepsilon_{zz}) + (q_x^2 + q_y^2 - k_0^2 \varepsilon_{zz}) (q_x^2 - k_0^2 \varepsilon_{xx}), \\ \text{Ad}_{12} &= q_x q_y (q_z^2 + q_x^2 + q_y^2 - k_0^2 \varepsilon_{zz}), \\ \text{Ad}_{13} &= q_x q_z (q_z^2 + q_x^2 + q_y^2 - k_0^2 \varepsilon_{xx}), \\ \text{Ad}_{22} &= q_z^2 (q_y^2 - k_0^2 \varepsilon_{zz}) + (q_x^2 + q_y^2 - k_0^2 \varepsilon_{zz}) (q_y^2 - k_0^2 \varepsilon_{xx}), \\ \text{Ad}_{23} &= q_y q_z (q_z^2 + q_x^2 + q_y^2 - k_0^2 \varepsilon_{xx}), \\ \text{Ad}_{33} &= (q_z^2 - k_0^2 \varepsilon_{xx}) (q_z^2 + q_x^2 + q_y^2 - k_0^2 \varepsilon_{xx}), \end{aligned} \quad (18)$$

where,  $\text{Ad}$  is symmetric. It is well known that  $D(\mathbf{q})$  is a polynomial of order four if  $q_z$  as shown in Eq.(17) and  $D(\mathbf{q})=0$  describes two wave normal surface[8]. The four poles of  $D(\mathbf{q})$  become real when  $\mathbf{q}$  is on the wave normal surface. In particular, two poles of  $D(\mathbf{q})$  are positive describing eigenmodes propagating in the positive  $z$ -direction. The other two are negative and they represent eigenmodes propagating in the negative  $z$ -direction. Otherwise, the poles are complex. The two poles in the upper complex plane are denoted as  $u^a$  and  $u^b$ , and the other two in the lower complex plane are denoted as  $u^c$  and  $u^d$ . Thus,  $k^a, k^b, k^c$  and  $k^d$  in Eq.(6) mean the diffracted wave vectors that represent ordinary wave propagating positive  $z$  direction, extraordinary wave propagating positive  $z$  direction, extraordinary wave propagating negative  $z$  direction and ordinary wave propagating negative  $z$  direction,

respectively for positive uniaxial crystal. We may call  $p^a, p^b, p^c$  and  $p^d$  phase matching term because  $[1 - e^{-iP_1^{a,b} d} / P_1^{a,b}]$  in Eq.(19) represent sinc function with respect to the variables  $P_1^{a,b}$ . This implies that  $P_1^{a,b}$  are the same as the phase matching function in the conventional coupled mode theory[5].  $\mathbf{K}_{tz}$  in Eq.(14) represents volume grating vector and  $\alpha_n$  in Eq.(16) is a second rank tensor that represents the volume grating magnitude.

### III. CROSS-TALK EFFECTS ANALYSIS

The formula presented in the above section is used to study various cross-talk effects arising from light diffraction from superposed volume gratings. In particular, the interconnection pattern of the input and output pixels shown in Fig. 2 is considered. The first order diffraction formula will justify the selection of the input and output pixels shown in Fig. 2 and it will also give the amplitude of the signal of each interconnection. Second order cross-talk is also considered. However, in a real situation, the second order cross-talk can be eliminated by choosing a specific medium and it will be explained. Finally, the third order cross-talk which yields the signal-to-noise ratio of the volume holographic interconnections will be considered.

#### III. A. First order cross-talk

Consider an input pixel  $i$  shown in Fig. 1. There

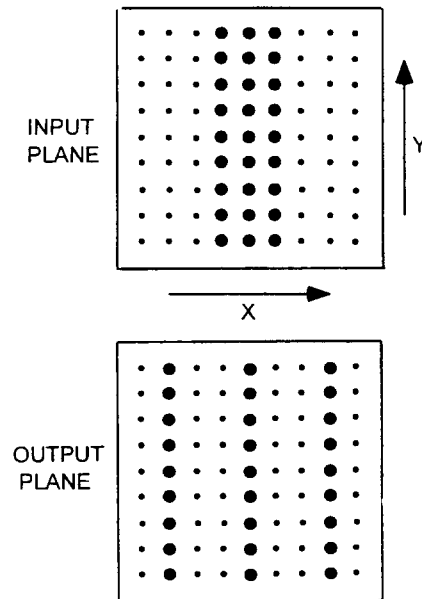


FIG. 2. A specific arrangement of input and output pixels on 9x9 rectangular grids which eliminates the first level cross-talk effect. Large dots on the input and output plane represent light sources and photodetectors, respectively.

are  $N^2$  total gratings representing the interconnection pattern, where  $N$  is the total number of input and output pixels used. The plane wave emanating from that pixel will interact with  $N^2$  gratings and the diffraction is described by the general formula derived in the above section. In the first level diffraction, it has been shown that the light wave interacts with each grating as if there is only one grating. Thus, there is no mixing due to multiple gratings. In Fig. 1, the input pixel  $\mathbf{i}$  is interconnected to every output pixel by  $N$  gratings and each of these  $N$  gratings yields the signal of the particular interconnection. Furthermore, the diffraction which yields the signal satisfies the Bragg condition exactly. Thus, using the general formula, the amplitude of the signal of each interconnection is given by

$$\begin{aligned} \mathbf{E}_{a,b}^{(1)}(\mathbf{r}) &= -\frac{1}{\epsilon_{zz}} \frac{\mathbf{A}(\mathbf{k}_1^{a,b})}{\prod_1^{a,b}} \cdot \frac{1 - e^{-iP_1^{a,b}d}}{P_1^{a,b}} \mathbf{E}_0 \exp(i\mathbf{k}_1^{a,b} \cdot \mathbf{r}) \\ &= -\frac{id}{\epsilon_{zz}} \frac{\mathbf{A}(\mathbf{k}_1^{a,b})}{\prod_1^{a,b}} \mathbf{E}_0 \exp(i\mathbf{k}_1^{a,b} \cdot \mathbf{r}), \end{aligned} \quad (19)$$

where the exact Bragg condition  $P_1^{a,b} = 0$  was used and the appropriate limit was taken. The amplitude of the signal depends on the light polarization, the anisotropy of the host material and gratings, the light propagation direction, and the arrangement of the gratings relative to the lights. All of these factors are reflected in Eq.(19). It is well known that if an input pixel  $\mathbf{i}'$  is in the same horizontal line as the input pixel  $\mathbf{i}$  in Fig. 1 (i.e.  $x$ -direction), the grating generated by a pair of pixels  $\mathbf{i}'$  and  $\mathbf{p}'$  yields extremely small magnitudes of phase mismatching when the light coming from input pixel  $\mathbf{i}$  interacts with this grating. Thus, the light wave emanating from the pixel  $\mathbf{i}$  interacts with these gratings very strongly and the amplitude is almost the same as that of Eq.(19). However, to ensure independent interconnections, these gratings should be ineffective. The specific pattern shown in Fig. 2 was chosen to ensure that the diffracted output waves from these gratings do not propagate to the used output pixels and thus, they are ineffective. The propagation direction from a single grating is given by Eq.(15) and it depends only on the  $x$  and  $y$  components of the light and grating wave vectors. This shows that indeed the selection of the input and output pixels in Fig. 2 eliminates the problem caused by the gratings in the horizontal direction. Then, if an input pixel  $\mathbf{i}'$  is in the same vertical line as the input pixel  $\mathbf{i}$  in Fig. 1 (i.e.  $y$ -direction), the grating generated by a pair of pixels  $\mathbf{i}'$  and  $\mathbf{p}'$  yields large magnitudes of phase mismatching when the angular separation between the pixel  $\mathbf{i}$  and  $\mathbf{i}'$  is large. The result is the well known angular selectivity of volume gratings. The magnitude of the diffracted light waves from these gratings follows from Eq.(19) as  $|\mathbf{E}_{a,b}^{(1)}(\mathbf{r})|^2 \approx \text{sinc}^2(P_1^{a,b} \cdot d/2)$  irrespective of polarization, anisotropy, and geometric configuration.

Thus, if  $|P_1^{a,b}|$  is close to  $2\pi$ , the effect of the above gratings can be ignored. Fig. 5 and Fig. 6 in the next section will justify the specific selection of the input and output pixels as shown in Fig. 2.

### III. B. Second order cross-talk

The desired interconnection is from the pixel  $\mathbf{i}$  to  $\mathbf{p}$ . Second order cross-talk effects result from light waves that are first diffracted by a grating  $\mathbf{K}_1$  from an input wave at pixel  $\mathbf{i}$ , and re-diffracted by a second grating  $\mathbf{K}_2$  and are directed to the output pixel  $\mathbf{p}$  as shown in Fig. 3. The amplitude of the second order cross-talk follows from Eqs.(6)-(16) after taking the limit for the case of the exact Bragg condition

$$\mathbf{E}_a^{(2)}(\mathbf{r}) = \frac{d^2}{(\epsilon_{zz})^2 2!} \frac{\mathbf{A}(\mathbf{k}_2^a) \mathbf{A}(\mathbf{k}_1^a)}{\prod_2^a \prod_1^a} \mathbf{E}_0 \exp(i\mathbf{k}_2^a \cdot \mathbf{r}). \quad (20)$$

The second order diffraction yields cross-talk effects because the diffraction may involve two different gratings simultaneously. The principal source of second order cross-talk effects is diffraction from the interlayer grating (i.e. interconnection grating  $K_1$  in Fig. 3) followed by re-diffraction from the intralayer grating (i.e.  $K_2$  generated by interfering two beams  $k_p$  and  $k_j$  in Fig. 3). It is desirable to minimize the strength of the intralayer grating to eliminate second order cross-talk. This can be accomplished by selecting a holographic recording medium in which low spatial frequencies are recorded weakly. This is, for instance, typical of gratings recorded in photorefractive crystals in the absence of an applied electric field, in which case the recording is done principally by diffusion of the carriers. In this case, gratings whose period is considerably longer than the diffusion length are not recorded effectively. As

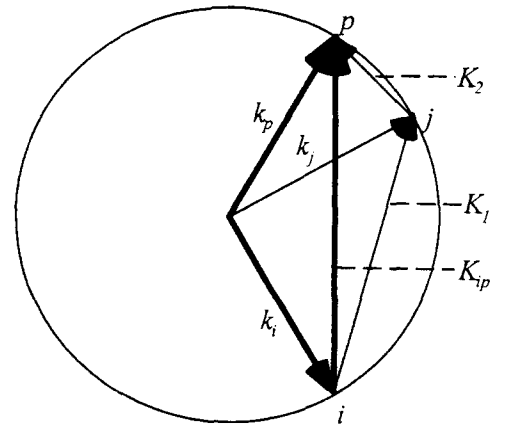


FIG. 3. A possible double diffraction which yields second order cross-talk to the interconnection between the input pixel  $\mathbf{i}$  and the output pixel  $\mathbf{p}$  due to two gratings  $\mathbf{K}_2$ , and  $\mathbf{K}_1$ .

an example, if  $\text{KNbO}_3 : \text{Fe}$  300 ppm is utilized[9], the diffraction efficiency for  $0.3[\mu\text{m}]$  fringe spacing is more than three orders of magnitude larger than  $2.6[\mu\text{m}]$ . Hence, if the specific medium and the arrangement of input and output pixels are chosen such that the spatial frequency of interlayer gratings is much higher than that of the intralayer gratings, then the effects of intralayer gratings can potentially be made negligible compared to third order cross-talk effects.

### III. C. Third order cross-talk

The third order cross-talk effects stems from the interaction of the light wave with triple gratings selected from a total of  $N^2$  gratings. An example of this triple diffraction is shown in Fig. 4. In that figure the desired interconnection is from the pixel  $i$  to the output pixel  $p$ . However, the third level diffraction caused by triple gratings represented by  $[\mathbf{K}_3, \mathbf{K}_2, \mathbf{K}_1, ]$  generates a light wave propagating to the same output pixel  $p$ . The input light wave at the pixel  $i$  first interacts with the grating  $\mathbf{K}_1$  and the diffracted light propagates to the pixel  $j$ . Then, the diffracted light wave interacts with the grating  $\mathbf{K}_2$  and the doubly diffracted light propagates to the pixel  $l$ . Finally, the doubly diffracted wave interacts with the grating  $\mathbf{K}_3$  and the triply diffracted light wave propagates to the pixel  $p$ . This third level diffracted light acts as cross-talk in the interconnection because the amplitude depends on the gratings  $\mathbf{K}_3, \mathbf{K}_2,$  and  $\mathbf{K}_1$ , which represent different interconnections. There may be a large number of triple gratings which can be selected from  $N^2$  gratings. However, the triple gratings that satisfy the Bragg condition exactly at the first, second and third intermediate diffraction step yield the strongest cross-talk effects. The example shown in Fig. 3 is one of such triple gratings. The

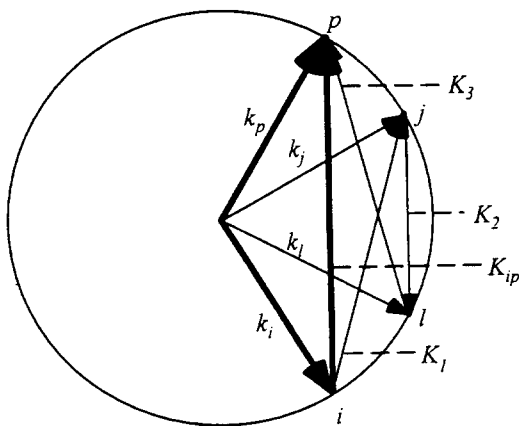


FIG. 4. A possible triple diffraction which yields third order cross-talk to the interconnection between the input pixel  $i$  and the output pixel  $p$  due to three gratings  $\mathbf{K}_3, \mathbf{K}_2,$  and  $\mathbf{K}_1$ .

amplitude of the light wave diffracted from each triple gratings is given by the general formula

$$\mathbf{E}_a^{(3)}(\mathbf{r}) = \frac{id^3}{(\epsilon_{zz})^3 3!} \frac{\mathbf{A}(\mathbf{k}_3^a)\mathbf{A}(\mathbf{k}_2^a)\mathbf{A}(\mathbf{k}_1^a)}{\prod_3^a \prod_2^a \prod_1^a}. \quad (21)$$

Total third order cross-talk noise of the volume holographic interconnection can be obtained by summing the result of Eq.(19) which are applied to each possible triple gratings selected from  $N^2$  gratings. The total number of possible triple gratings for the specific arrangement of input and output pixels was obtained previously[2].

### IV. EXAMPLES OF NUMERICAL CALCULATION

In the following, we select several examples and present numerical results obtained by applying the general formula. For simplicity, a uniaxial crystal with its optic axis coincident with the  $z$ -direction is considered. In all calculations,  $k_0 = 2\pi/\lambda, \lambda = 514.5 \times 10^{-9}, n_o = 2.3, n_e = 2.21, d = 1\text{cm}$  and the Bragg angle is chosen as 30 degrees. All the components of grating strength are assumed  $5 \times 10^{-6}$ . We assume that the input wave is a unit amplitude plane wave. Fig. 5 and Fig. 6 show the diffracted output wave intensity versus horizontal deviation angle and vertical deviation angle from the Bragg angle for the first level diffraction when interacting with one grating  $\mathbf{K}$  laid on the  $x$ - $z$  plane. Fig. 5 and Fig. 6 describe well the specific selection of the input and out pixels as shown in Fig 2. Fig. 7 shows the diffracted output wave intensity versus vertical deviation angle from the Bragg angle for the third level diffraction that having  $[\mathbf{K}, -\mathbf{K}, \mathbf{K}]$  diffraction sequence, and the grating  $\mathbf{K}$  also laid on the  $x$ - $z$  plane. As shown in Fig. 7, the third level

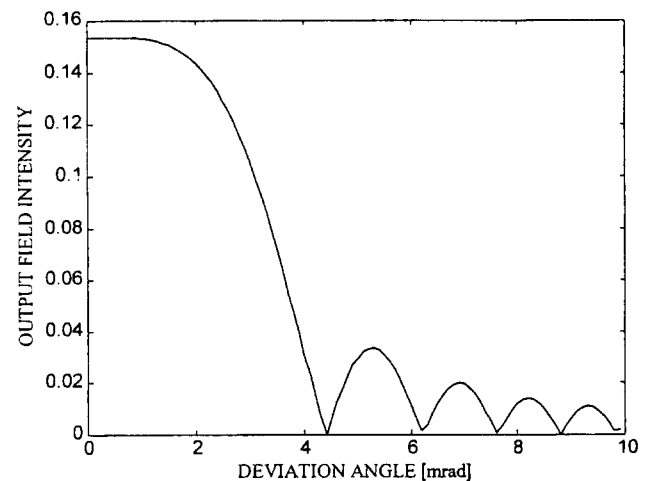


FIG. 5. Variation for the first level diffracted output wave intensity versus horizontal deviation angle

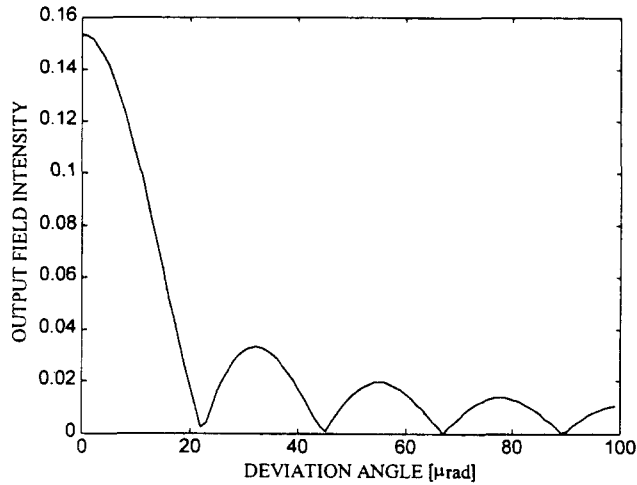


FIG. 6. Variation for the first level diffracted output wave intensity versus vertical deviation angle

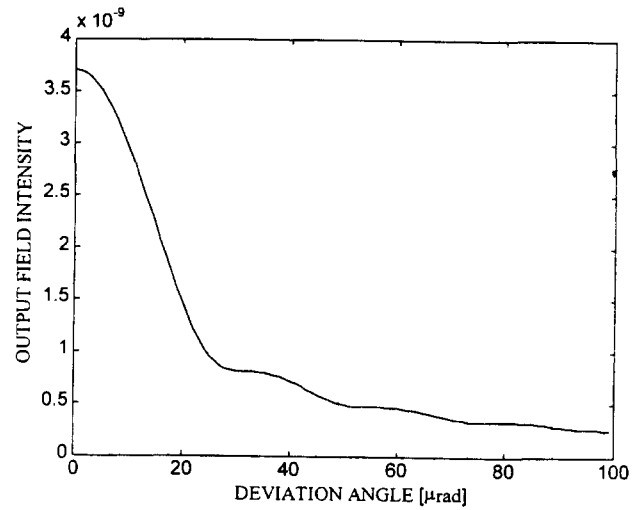


FIG. 8. Variation for the third level diffracted output wave intensity due to the back-scattering effect versus vertical deviation angle

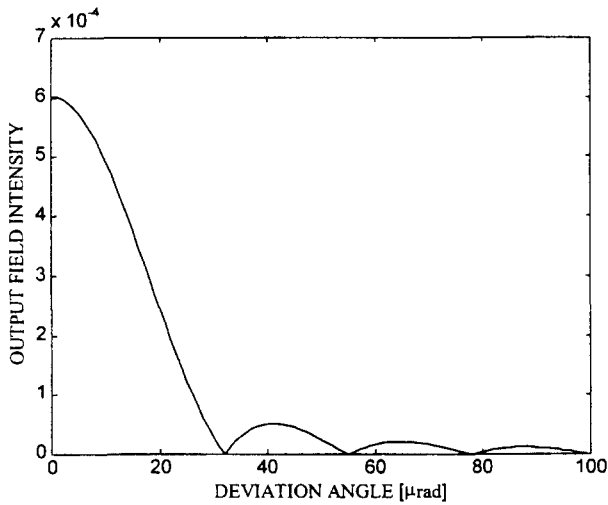


FIG. 7. Variation for the third level diffracted output wave intensity versus vertical deviation angle

diffraction which has  $\beta_3 = a, \beta_2 = a, \beta_1 = a$  sequence and has  $\alpha_1 = \alpha_2 = \alpha_3$  grating strength, is very small compared to the first level diffraction. Fig. 8 shows the third level diffraction due to the back-scattering effect, which has  $\beta_3 = a, \beta_2 = d, \beta_1 = a$  sequence for the same situation as in Fig. 7.

## V. CONCLUSIONS

The integral expansion method of the Maxwell's equation was applied to analyze various cross-talk effects arising from superposed volume gratings for arbitrary light polarization, interaction geometry, and anisotropy of the host materials. Some numerical results using general formula are given for first and third order diffraction.

## REFERENCES

- [1] D.Psaltis, X.G.Gu, and H.Lee, Tech.Digest, Topical Meeting Opt.Com., Lake Tahoe, 129 (1987)
- [2] H.Lee, X.G.Gu, and D.Psaltis, J.Appl.Phys. **65**, 2191 (1989)
- [3] P.Van Heerden, Appl. Opt. **2**, 387 (1963)
- [4] H.Lee, Opt. Lett. **13**, 874 (1988)
- [5] H.Kogelnik, Bell Syst. Tech. J. **48**, 2909 (1968)
- [6] E.N.Glytsis and T.K.Gaylord, Appl. Opt. **28**, 2401 (1989)
- [7] S.K.Jin, Ph.D. Thesis, Seoul National Univ., (1994)
- [8] S.K.Jin, J. Opt. Soc. Korea. **1**, 67 (1997)
- [9] P.Gunter, phys.Rep. **93**, 199(1982)